UCLA
COMPUTATIONAL AND APPLIED MATHEMATICS

# The Gaussian Moment Closure for Gas Dynamics

C. David Levermore
William J. Morokoff

February 1996

CAM Report 96-4

Department of Mathematics
University of California, Los Angeles
Los Angeles, CA. 90024-1555

*SIAM J. on Applied Mathematics*, submitted 20 February 1996

# The Gaussian Moment Closure for Gas Dynamics

C. David Levermore

*Department of Mathematics*
*and*
*Program in Applied Mathematics*
*University of Arizona, Tucson, AZ 85721*
lvrmr@math.arizona.edu

William J. Morokoff

*Department of Mathematics*
*University of California, Los Angeles*
*Los Angeles, CA 90095-1555*
morokoff@math.ucla.edu

## Abstract

The moment closure method of Levermore applied to the Boltzmann equation for rarefied gas dynamics leads to a hierarchy of symmetric hyperbolic systems of partial differential equations. The Euler system is the first member of this hierarchy of closures. In this paper we investigate the next member, the ten moment Gaussian closure. We first reduce the collision term to an integral which may be explicitly evaluated for the special case of Maxwell molecular interaction. The resulting collision term for this case is shown to be equivalent to the term obtained by replacing the Boltzmann collision operator with the BGK approximation. We then analyze the Gaussian system applied to the canonical flow problem of a stationary planar shock. An analytic shock profile for the Gaussian closure is derived and compared with the numerical solutions of the Boltzmann and Navier-Stokes equations. The results show reasonable agreement for weak shocks and close agreement between the downstream Gaussian and Navier-Stokes profiles. The results also suggest what may be expected from higher moment closure systems. In particular, the presence of discontinuities in the solution are seen not to prohibit the development of significant profiles.

# 1. INTRODUCTION

The computation of extremely low pressure rarefied gas flows is important in a wide range of applications, from the reentry of space vehicles to the design of manufacturing equipment for semiconductor chips. The appropriate mathematical description of such flows is given by the Boltzmann equation, which describes the evolution of the one particle velocity distribution function. The mathematical and computational difficulties associated with this equation are well known. It is therefore of interest to consider approximating fluid dynamic systems which are related to velocity moments of the Boltzmann equation.

The simplest such system is the Euler equations, which are based on the assumption that the gas is in local thermodynamic equilibrium. An asymptotic expansion about this equilibrium following the Chapman-Enskog procedure leads to the Navier-Stokes equations. The validity of the Navier-Stokes system becomes questionable as the expansion parameter ceases to be small, however. This is related to the fact that the underlying velocity distribution function for the Navier-Stokes system is not everywhere nonnegative. As the gas moves away from equilibrium, the momentum and energy fluxes predicted by the Navier-Stokes equations may be off by orders of magnitude.

An alternative approach to the asymptotic expansion was proposed by Grad [10]. He considered using a 13 moment closure as opposed to the five moments of Euler and Navier-Stokes (mass, energy and three for momentum). The closure of this system, based on setting higher moments to zero, led to a system of equations which were not always hyperbolic. More recently, a procedure was developed by Levermore [12] that generates a hierarchy of moment closure systems, each of which possesses an entropy and is symmetric hyperbolic. The simplest member of this hierarchy is the Euler system, which has five equations. In this paper we investigate the next member, the Gaussian closure system, which has ten equations. This system is considerably simpler than subsequent members of the hierarchy, which makes it an ideal tool studying phenomena that arise in these systems. The presence of nontrivial viscous stress introduces important physical features not found in the Euler system. In partiuclar, we will investigate the way in which collisional effects are modeled and the nature of shock profiles. We remark, however, that the absence of heat flux in the Gaussian system makes it of limited use as a practical modeling tool.

This paper is organized as follows. In Section 2 after a brief review of the closure procedure of [12], the Gaussian closure system is derived. For the classical Boltzmann collision operator the collision term in the Gaussian system reduces to an integral over $\mathbb{R}^3$ generally, and to an integral over over the unit sphere $\mathbb{S}^2$ for many commonly used molecular interaction models. Some details of this reduction are relegated to an appendix. For the case of Maxwell molecules, this integral may be explicitly evaluated. The resulting collision term is shown to be equivalent to the term obtained by replacing the Boltzmann collision operator with the BGK approximation. In Section 3 the Gaussian system is analyzed for the case of a steady planar shock profile. An exact analytic solution is found which is compared to numerical solutions of the Boltzmann and Navier-Stokes equations. Finally, some conclusions concerning the applicability of moment closure systems are drawn.

## 2. THE GAUSSIAN CLOSURE

### 2.1. Moment Closure Equations

The moment closure procedure of [12] considers general kinetic equations that describe the evolution of a one particle velocity distribution function $F(t,x,v)$, which in three dimensions is a function of the seven independent variables $(t,x,v) \in \mathbb{R}_+ \times \mathbb{R}^3 \times \mathbb{R}^3$. For neutral particles in the absence of external forces the equations considered have the form

$$\partial_t F + v \cdot \nabla_x F = \mathcal{C}(F)\,. \tag{2.1}$$

Here the collision operator $F \mapsto \mathcal{C}(F)$ acts only on the $v$ dependence of $F$ locally at each $(t,x)$ and describes the rate of change of $F$ due to collisions. It contains the microscopic interaction laws from which macroscopic quantities such as viscosity and thermal conductivity may be derived. In the study of such equations, integration over velocity space often arises. We therefore find it convenient to introduce the notation

$$\langle f \rangle = \int_{\mathbb{R}^3} f(v)\, d^3v \tag{2.2}$$

for any scalar- or vector-valued function $f = f(v)$.

The collision operator $\mathcal{C}$ is assumed to possess several important properties. First, it is assumed to have 1, $v$ and $|v|^2$ as locally conserved quantities, which means that

$$\langle \mathcal{C}(f) \rangle = 0\,, \qquad \langle v\, \mathcal{C}(f) \rangle = 0\,, \qquad \langle |v|^2 \mathcal{C}(f) \rangle = 0\,, \tag{2.3}$$

for every $f$ for which these expressions are defined. Moreover, it can be shown that every other locally conserved quantity is a linear combination of these, so that for any $g = g(v)$ the following statements are equivalent:

$$\begin{aligned} &\text{i)} \quad \langle g\, \mathcal{C}(f) \rangle = 0 \quad \text{for every } f\,, \\ &\text{ii)} \quad g \in \mathbb{E} \equiv \operatorname{span}\{1, v_x, v_y, v_z, |v|^2\}\,. \end{aligned} \tag{2.4}$$

Second, the operator $\mathcal{C}$ is assumed to satisfy the local entropy dissipation relation

$$\langle \log f\, \mathcal{C}(f) \rangle \leq 0 \quad \text{for every } f\,. \tag{2.5}$$

In addition, the vanishing of the quantity on the left characterizes the local equilibria of $\mathcal{C}$, and these equilibria are given by the class of Maxwellian densities, i.e. those of the form

$$f = \mathcal{E}(\rho, u, \theta) \equiv \frac{\rho}{(2\pi\theta)^{\frac{3}{2}}} \exp\left( - \frac{|v-u|^2}{2\theta} \right), \tag{2.6}$$

for some $(\rho, u, \theta) \in \mathbb{R}_+ \times \mathbb{R}^3 \times \mathbb{R}_+$. More precisely, for every $f$ for which $\mathcal{C}(f)$ is defined, the following statements are equivalent:

$$\begin{aligned} &\text{i)} \quad \langle \log f \, \mathcal{C}(f) \rangle = 0 \,, \\ &\text{ii)} \quad \mathcal{C}(f) = 0 \,, \\ &\text{iii)} \quad f \text{ is a Maxwellian density given by (2.6).} \end{aligned} \tag{2.7}$$

Finally, the operator $\mathcal{C}$ is assumed to be Galilean invariant; namely, it is assumed to commute with the action of translational and orthogonal transformations on $v$.

Solutions of kinetic equations like (2.1) are generally difficult to simulate because of the seven independent variables involved and the complexity of the collision operator, which is usually nonlocal in the velocity variable $v$. For this reason it is natural to consider approximating systems of equations that are obtained by integrating out $v$. If $\boldsymbol{m}(v)$ is a vector whose elements are polynomials in the components of the velocity $v = (v_x, v_y, v_z)$, then a system of equations for the moments $\langle \boldsymbol{m} F \rangle$ may be obtained from (2.1) as

$$\partial_t \langle \boldsymbol{m} F \rangle + \nabla_x \cdot \langle v \boldsymbol{m} F \rangle = \langle \boldsymbol{m} \mathcal{C}(F) \rangle \,. \tag{2.8}$$

This system however is not closed because the integration of $\boldsymbol{m}(v)$ against $vF$ introduces moments of $F$ that cannot be expressed in terms of the moments $\langle \boldsymbol{m} F \rangle$. Formal closures for (2.8) may be obtained by choosing a specific functional form for $F = F(v)$ that depends on parameters which are taken to be functions of $t$ and $x$, where there are as many parameters as there as moment equations. For example, if $\boldsymbol{m} = (1, v_x, v_y, v_z, |v|^2)^T$ and $F$ is taken to have the form of a local Maxwellian equilibrium $\mathcal{E}(\rho, u, \theta)$ given by (2.6), then (2.8) becomes the Euler equations of gas dynamics.

A systematic procedure was given in [12] for selecting moment vectors $\boldsymbol{m}$ and corresponding distribution functions $F$ which yields a hierarchy of closures for (2.8), each member of which is a symmetric hyperbolic system with entropy. A key necessary (although not the only) condition on $\boldsymbol{m}$ is that the highest degree of its polynomial elements must be even. Once an appropriate $\boldsymbol{m}$ is chosen, the family of distribution functions is taken to be

$$F = \exp\bigl(\boldsymbol{\alpha}^T \boldsymbol{m}(v)\bigr) \,, \tag{2.9}$$

where the parameters $\boldsymbol{\alpha}$ are functions of $t$ and $x$. Equations (2.8) then become a system for $\boldsymbol{\alpha} = \boldsymbol{\alpha}(t, x)$. The members of this hierarchy are ordered by containment of the linear spans of the components of $\boldsymbol{m}$.

The simplest member of this moment closure hierarchy corresponds to the choice of moment vector $\boldsymbol{m} = (1, v, |v|^2)^T$, by which we denote the five dimensional vector whose components consist of the scalar 1, the three components of $v$, and the scalar $|v|^2$. The corresponding family of distribution functions prescribed by (2.9) is equivalent to the Maxwellians $\mathcal{E}(\rho, u, \theta)$ given by (2.6), which may be expressed in terms of the $\boldsymbol{\alpha}$ through the invertible relation

$$\boldsymbol{\alpha} = \left( \log\left( \frac{\rho}{(2\pi\theta)^{3/2}} \right) - \frac{|u|^2}{2\theta} \,, \, \frac{u}{\theta} \,, \, -\frac{1}{2\theta} \right)^T . \tag{2.10}$$

This so-called Maxwellian closure therefore yields the familiar system of Euler equations of gas dynamics.

The next simplest member of the moment closure hierarchy corresponds to the choice of moment vector $\boldsymbol{m} = (1, v, v \vee v)^T$. Here $\vee$ denotes the symmetric tensor outer product which generally acts on a symmetric $k$-tensor and a symmetric $l$-tensor by symmetrizing their usual tensor outer product. In particular, $v \vee v$ can be thought of as the symmetric matrix $v \vee v = vv^T$, which has six independent components. Hence, $(1, v, v \vee v)^T$ denotes the ten dimensional vector whose components consist of the scalar 1, the three components of $v$, and the six components of $v \vee v$. The corresponding family of distribution functions prescribed by (2.9) is equivalent the Gaussian distributions over $v$, which are parametrized by their weight $\rho$, mean $u$, and variance $\Theta$, and are given by

$$\mathcal{G}(\rho, u, \Theta) = \frac{\rho}{\sqrt{\det(2\pi\Theta)}} \exp\big( -\tfrac{1}{2}(v-u)^T \Theta^{-1}(v-u)\big)\,. \tag{2.11}$$

Here, as with the Maxwellians, $\rho$ and $u$ are identified with the fluid mass density and stream velocity. The new feature is that the scalar temperature $\theta$ has been replace by the symmetric positive definite matrix $\Theta$. As was the case with the Maxwellians, the Gaussians $\mathcal{G}(\rho, u, \Theta)$ may be expressed in terms of the $\boldsymbol{\alpha}$ through the invertible relation

$$\boldsymbol{\alpha} = \left( \log\left( \frac{\rho}{\sqrt{\det(2\pi\Theta)}} \right) - \tfrac{1}{2} u^T \Theta^{-1} u \,,\, \Theta^{-1} u \,,\, -\tfrac{1}{2}\Theta^{-1} \right)^T . \tag{2.12}$$

The so-called Gaussian closure yields moment equations (2.8) that may be written in terms of the variables $(\rho, u, \Theta)$ as

$$\partial_t \rho + \nabla_x \cdot \big(\rho u\big) = 0\,, \tag{2.13a}$$

$$\partial_t \big(\rho u\big) + \nabla_x \cdot \big(\rho u \vee u + \rho\Theta\big) = 0\,, \tag{2.13b}$$

$$\partial_t \big(\rho u \vee u + \rho\Theta\big) + \nabla_x \cdot \big(\rho u \vee u \vee u + 3\rho\Theta \vee u\big) = \Xi(\rho, \Theta)\,, \tag{2.13c}$$

where the collisional term $\Xi$ is shown to be independent of $u$ by first using the translation invariance and then using local conservation (2.3) to obtain

$$\begin{aligned} \Xi(\rho, \Theta) &\equiv \langle v \vee v\, \mathcal{C}(\mathcal{G}(\rho, 0, \Theta))\rangle \\ &= \langle (v-u) \vee (v-u)\, \mathcal{C}(\mathcal{G}(\rho, u, \Theta))\rangle \\ &= \langle v \vee v\, \mathcal{C}(\mathcal{G}(\rho, u, \Theta))\rangle\,. \end{aligned} \tag{2.14}$$

We shall refer to system (2.13) as the Gaussian closure system.

The relation of the Gaussian to the Maxwellian closure may be brought out more clearly if we associate a scalar temperature $\theta$ with the variance matrix $\Theta$ by $\theta = \frac{1}{3}\mathrm{tr}(\Theta)$, where $\mathrm{tr}(\,\cdot\,)$ denotes the trace operation. By taking the trace of (2.13c), the scalar conservation of energy law may be expressed as

$$\partial_t\big(\rho|u|^2 + 3\rho\theta\big) + \nabla_x\cdot\big(\rho|u|^2 u + 3\rho\theta u + 2\rho\Theta u\big) = 0\,. \tag{2.15}$$

Note that when $\Theta = \theta I$ ($I$ being the identity matrix), $\mathcal{G}(\rho, u, \Theta) = \mathcal{E}(\rho, u, \theta)$ and equations (2.13a), (2.13b) and (2.15) reduce to the Euler system obtained from the Maxwellian closure.

An important observation about the system (2.13) is that if the initial data for $\Theta$ is symmetric positive definite, then it remains so. This may be seen by rewriting equation (2.13c) as a Langrangian equation for the temperature evolution

$$\big(\partial_t + u\cdot\nabla_x\big)\Theta + \big(\Theta\cdot\nabla_x u + (\nabla_x u)^T\cdot\Theta\big) = \frac{1}{\rho}\Xi(\rho,\Theta)\,. \tag{2.16}$$

This equation and the symmetry of $\Xi$ show that the evolution of $\Theta$ is consistent with it remaining a symmetric matrix. The fact that $\Theta$ remains positive definite may be seen by multiplying (2.16) on the left by $\Theta^{-1}$ and taking the trace. Upon using the identity $\partial_s \log(\det(\Theta)) = \mathrm{tr}(\Theta^{-1}\partial_s\Theta)$ and the conservation of mass (2.13a), it follows that

$$\big(\partial_t + u\cdot\nabla_x\big)\log\!\left(\frac{\det(\Theta)}{\rho^2}\right) = \frac{1}{\rho}\,\mathrm{tr}\big(\Theta^{-1}\Xi(\rho,\Theta)\big) \geq 0\,. \tag{2.17}$$

The inequality is a consequence of the entropy dissipation relation (2.5). It follows from (2.17) that $\det(\Theta)$ never passes through zero as long as $\rho$ remains positive. Hence, its eigenvalues remain bounded away from zero, and $\Theta$ remains positive definite.

It is also important to note that for the Gaussian closure system (2.13), the stress tensor $\Sigma$ (related to the momentum flux) and the heat flux vector $q$ are given by

$$\begin{aligned}\Sigma &= \Big\langle\Big((v-u)\vee(v-u) - \tfrac{1}{3}|v-u|^2 I\Big)\,\mathcal{G}\Big\rangle = \rho\,(\Theta - \theta I)\,,\\ q &= \big\langle\tfrac{1}{2}|v-u|^2(v-u)\,\mathcal{G}\big\rangle = 0\,.\end{aligned} \tag{2.18}$$

For the Euler system both of these quantities are identically zero. From (2.18) it is clear that away from equilibrium (i.e., where $\Theta \neq \theta I$) nonzero stresses may arise. This indicates that the Gaussian closure will give rise to viscous effects not present in the Euler equations. On the other hand, the heat flux vector vanishes identically for both the Maxwellian and Gaussian closures. This suggests that when stress effects dominate, the Gaussian closure will present a more accurate model than the Euler equations; however, both breakdown when heat flux effects become significant.

## 2.2. Collision Term for the Boltzmann Equation

We will now restrict the analysis here to the classical Boltzmann collision operator which describes the changes in $F$ due to binary collisions. For particles of mass $m$ it has the form

$$C(F)(v) = \frac{1}{m}\int_{\mathbb{R}^3}\int_{\mathbb{S}^2_+}\Big(F(v')F(w') - F(v)F(w)\Big)\,B(|v-w|,\eta)\,d^2\hat{n}\,d^3w\,, \tag{2.19}$$

where the unit vector $n$ is integrated over the unit half sphere $\mathbb{S}^2_+$ with azimuthal direction determined by $v-w$. The cosine $\eta \in [0,1]$ is defined by $(v-w)\cdot n = |v-w|\eta$. The post-collision velocities $v'$ and $w'$ are related to the pre-collision velocities $v$ and $w$ by

$$v' = v - n\big(n\cdot(v-w)\big)\,, \qquad w' = w + n\big(n\cdot(v-w)\big)\,. \tag{2.20}$$

The positive function $B(|v-w|,\eta)$ is the collision kernel and has units of $[length]^3[time]^{-1}$. It describes the nature of the two particle interaction and may be derived from an inter-particle potential [6]. It contains the microscopic interaction laws from which macroscopic quantities such as viscosity and thermal conductivity may be derived.

When the general definition (2.14) of the collision term $\Xi(\rho,\Theta)$ is applied with the Boltzmann collision operator (2.19), one obtains the integral expression for $\Xi$ given by

$$\Xi(\rho,\Theta) = \frac{1}{m}\int_{\mathbb{R}^3}\int_{\mathbb{R}^3}\int_{\mathbb{S}^2_+} v\vee v\Big(\mathcal{G}(v')\mathcal{G}(w') - \mathcal{G}(v)\mathcal{G}(w)\Big)B\,d^2\hat{n}\,d^3w\,d^3v\,, \tag{2.21}$$

where $\mathcal{G}(v) = \mathcal{G}(\rho,0,\theta)$ is given by (2.11). In the appendix it is shown that this eight-fold integral can be reduced to

$$\Xi(\rho,\Theta) = \frac{\rho^2}{m\sqrt{\det(4\pi\Theta)}}\int_{\mathbb{R}^3}\big(|v|^2 I - 3v\vee v\big)\,\xi(|v|)\,\exp\Big(-\tfrac{1}{4}v^T\Theta^{-1}v\Big)\,d^3v\,, \tag{2.22}$$

where the scalar-valued function $\xi(|v|)$ is given by

$$\xi(|v|) = \pi\int_0^1\big(\eta^2-\eta^4\big)\,B(|v|,\eta)\,d\eta\,. \tag{2.23}$$

Hence, all the information from the collision kernel $B(|v_r|,\eta)$ is contained in $\xi(|v|)$, which, by (2.23), is independent of $\Theta$.

The structure of (2.22) may be further exposed by a change to spherical coordinates in the integral. If we introduce the radial variable $c = |v|$ and the unit vector $n = v/c$, so that $d^3v = c^2\,dc\,d^2\hat{n}$, then (2.22) takes the form

$$\Xi(\rho,\Theta) = \frac{\rho^2}{m\sqrt{\det(4\pi\Theta)}}\,S(\Theta)\,, \tag{2.24}$$

where $S(\Theta)$ is the matrix-valued function

$$S(\Theta) = \int_{\mathbb{S}^2} (I - 3n\vee n)\; s\big(n^T\Theta^{-1}n\big)\, d^2\hat{n}\,, \tag{2.25}$$

which is defined in terms of the positive scalar-valued function

$$s(Z) = \int_0^\infty \exp\big(-\tfrac{1}{4}Zc^2\big)\,\xi(c)\,c^4\,dc\,. \tag{2.26}$$

It is evident from (2.25) that the matrix $S(\Theta)$ is symmetric and traceless.

Next we let $(\theta_1,\theta_2,\theta_3)$ be the eigenvalues of the matrix $\Theta$ and $Q$ be the orthogonal matrix which diagonalizes $\Theta$. Also let $(\eta_1,\eta_2,\eta_3)$ be the direction cosines of the unit vector $n$ along the eigenvectors of $\Theta$ that make up the columns of $Q$. Hence, we have

$$Q^T\Theta Q = \begin{pmatrix} \theta_1 & 0 & 0 \\ 0 & \theta_2 & 0 \\ 0 & 0 & \theta_3 \end{pmatrix}, \qquad Q^T n = \begin{pmatrix} \eta_1 \\ \eta_2 \\ \eta_3 \end{pmatrix}. \tag{2.27}$$

Then by (2.25) the matrix $S(\Theta)$ satisfies

$$\begin{aligned} Q^T S(\Theta) Q &= \int_{\mathbb{S}^2} \begin{pmatrix} 1-3\eta_1^2 & -3\eta_1\eta_2 & -3\eta_1\eta_3 \\ -3\eta_2\eta_1 & 1-3\eta_2^2 & -3\eta_2\eta_3 \\ -3\eta_3\eta_1 & -3\eta_3\eta_2 & 1-3\eta_3^2 \end{pmatrix} s\Big(\frac{\eta_1^2}{\theta_1}+\frac{\eta_2^2}{\theta_2}+\frac{\eta_3^2}{\theta_3}\Big)\, d^2\hat{n} \\ &= \int_{\mathbb{S}^2} \begin{pmatrix} 1-3\eta_1^2 & 0 & 0 \\ 0 & 1-3\eta_2^2 & 0 \\ 0 & 0 & 1-3\eta_3^2 \end{pmatrix} s\Big(\frac{\eta_1^2}{\theta_1}+\frac{\eta_2^2}{\theta_2}+\frac{\eta_3^2}{\theta_3}\Big)\, d^2\hat{n}\,. \end{aligned} \tag{2.28}$$

The integral of every off-diagonal entry above vanishes because the integrands have odd symmetry. It is clear from the form of this expression that if one could evaluate any one of the integrals on the diagonal, the evaluation other two integrals will follow by symmetry. As (2.28) shows, $Q$ diagonalizes $S(\Theta)$. Therefore, by (2.24), $Q$ diagonalizes $\Xi(\rho,\Theta)$ as well. Hence, while $\Xi(\rho,\Theta)$ does not generally take a simple form, it does have the property that it commutes with $\Theta$. For a general $\Theta$ this means that $\Xi(\rho,\Theta)$ must be a traceless linear combination of the matrices $I$, $\Theta$ and $\Theta^2$ with scalar coefficients that are symmetric functions of $(\theta_1,\theta_2,\theta_3)$.

Additional simplification is realized when the collision kernel $B$ takes the form

$$B(|v|,\eta) = \beta(\eta)\left(\frac{|v|}{\sqrt{\theta_{\rm ref}}}\right)^\gamma. \tag{2.29}$$

Here $\theta_{\rm ref}$ is an arbitrary reference temperature used to nondimensionalize $v$. Like $B(|v|,\eta)$, the function $\beta(\eta)$ has units of $[length]^3[time]^{-1}$. The parameter $\gamma$ plays the dominant role

in determining the transport properties of the model. It ranges from $\gamma = 0$ for Maxwell molecules to $\gamma = 1$ for hard spheres. Within this range the Boltzmann collision operator (2.19) possesses all the properties that were assumed in (2.3) through (2.7) [6].

The model (2.29) for $B$ is of interest for several reasons. First, it is exact with $\gamma = 1 - 4/p$ for inverse power law interparticle potentials of the form $\Phi(r) \propto r^{-p}$, where $p$ ranges from $p = 4$ for Maxwell molecules to $p \to \infty$ for hard spheres. In such a case $\beta(\eta)$ will have a singularity at $\eta = 0$ such that

$$\beta(\eta) = O\left(\eta^{-\frac{p+2}{p}}\right) \qquad \text{as } \eta \to 0, \tag{2.30}$$

unless an angular cut-off is imposed [6]. Second, with an appropriate choice of parameter $\gamma$ and function $\beta(\eta)$, not necessarily arising from an inverse power law potential, this model provides an accurate description of the true physical behavior of most pure species, at least over a limited temperature range. Finally, the standard Monte Carlo method used to numerically solve the Boltzmann equation [1] generally makes use of computational scattering angle models of the form (2.29), a comparison of which can be found in [15].

For the model (2.29), the function $\xi(|v|)$ defined by (2.23) takes the form

$$\xi(|v|) = \kappa \left(\frac{|v|}{\sqrt{\theta_{\text{ref}}}}\right)^{\gamma}, \tag{2.31}$$

where $\kappa$ is the positive constant with units of $[length]^3[time]^{-1}$ determined by the integral

$$\kappa = \pi \int_0^1 \left(\eta^2 - \eta^4\right) \beta(\eta)\, d\eta\,. \tag{2.32}$$

Notice that because this integral converges for a singularity such as (2.30), an angular cutoff is not needed to make sense of the Gaussian closure system when model (2.29) derives from an inverse power law interparticle potential. For model (2.29), or any other model for which $\xi(|v|)$ takes the form (2.31), the integral that defines $s(Z)$ in (2.26) can be expressed in terms of the classical $\Gamma$-function, whereby

$$s(Z) = \kappa\, \theta_{\text{ref}}^{\frac{5}{2}}\, 2^{4+\gamma}\, \Gamma\left(\tfrac{5+\gamma}{2}\right) \left(\theta_{\text{ref}}\, Z\right)^{-\frac{5+\gamma}{2}}\,. \tag{2.33}$$

We note, however, that even when $s(Z)$ has this simple form, the two-fold integrals that remain to be evaluated in (2.28) do not generally have representations in terms of elementary functions of $(\theta_1, \theta_2, \theta_3)$. Therefore (2.24) is the simplest representation of $\Xi(\rho, \Theta)$ available, where the entries of $S(\Theta)$ may be evaluated by (2.28).

### 2.3. Transport Coefficients and the BGK Approximation

We now address two problems associated with the collision term for general moment closure systems by considering solutions in the framework of the Gaussian closure. We first

consider the more subtle of these two difficulties. The problem here lies in the transport coefficients associated with the fluid dynamic limit. It is desirable that in this limit, in which the velocity distribution function $F$ approaches a Maxwellian distribution $\mathcal{E}$ (2.6), the viscosity and thermal conductivity of the moment closure system match the true physical values obtained from the Chapman-Enskog expansion for the full Boltzmann equation [6].

The Chapman-Enskog procedure for the Gaussian closure involves expanding the temperature matrix $\Theta$ about its equilibrium value $\theta I$. The result is that near local equilibrium we have

$$\Xi(\rho, \Theta) = \rho^2 \lambda(\theta)(\theta I - \Theta) + O\big(|\theta I - \Theta|^2\big)\,, \tag{2.34}$$

where $|\cdot|$ indicates any matrix norm, and $\lambda(\theta) > 0$ is computed by comparing a direct linearization of (2.22) via (2.24) and (2.28) to (2.34). We then obtain the result

$$\lambda(\theta) = -\frac{1}{m\, 5\pi^{\frac{1}{2}} \theta^{\frac{7}{2}}}\, s'\!\left(\frac{1}{\theta}\right). \tag{2.35}$$

When $B(|v|, \eta)$ has the form (2.29) then (2.35) simplifies to

$$\lambda(\theta) = \frac{\kappa\, 2^{4+\gamma}\, \Gamma\big(\frac{7+\gamma}{2}\big)}{m\, 5\pi^{\frac{1}{2}}} \left(\frac{\theta}{\theta_{\text{ref}}}\right)^{\frac{\gamma}{2}}. \tag{2.36}$$

As was shown in [12], the viscosity $\mu_{_G} = \mu_{_G}(\theta)$ given by the Chapman-Enskog procedure for the Gaussian closure is

$$\mu_{_G}(\theta) = \frac{\theta}{\lambda(\theta)}\,. \tag{2.37}$$

As was discussed in [12], the viscosity $\mu_{_G}$ is equal to the true viscosity $\mu$ (derived from the full Boltzmann equation) for Maxwell molecules, but is generally smaller than the true viscosity.

A comparison of $\mu_{_G}$ with the Sonine polynomial expansion of $\mu$ [7] shows that $\mu_{_G}$ is in fact identical to the first term of the expansion, which is often refered to as the first approximation to the viscosity. When $B(|v|, \eta)$ has the form (2.29) then (2.37) becomes

$$\mu_{_G}(\theta) = \frac{5\pi^{\frac{1}{2}}\, m\, \theta_{\text{ref}}}{\kappa\, 2^{4+\gamma}\, \Gamma\big(\frac{7+\gamma}{2}\big)} \left(\frac{\theta}{\theta_{\text{ref}}}\right)^{1-\frac{\gamma}{2}}. \tag{2.38}$$

A direct scaling argument shows that the true viscosity $\mu$ has the same functional dependence on $\theta$ as $\mu_{_G}$, and thus the two differ at most by the coefficient of proportionality. For $\gamma = 0$ (Maxwell molecules), these coefficients of $\mu_{_G}$ and $\mu$ are equal. As the collision interaction becomes harder, the deviation of these coefficients increases until for $\gamma = 1$ (hard spheres) the $\mu$ is around 1.6% larger than $\mu_{_G}$ [7]. For most real gases modeled by (2.29) the approximation $\mu_{_G}$ will be within about one percent of the true viscosity $\mu$. For

many engineering applications, this provides sufficient accuracy. Moreover, the viscosity is usually treated as a quantity obtained from experimental measurements to which the parameters $\kappa$ and $\gamma$ associated with the collision kernel (2.29) may be fit so that the viscosity of the Gaussian closure $\mu_G$ will match the experimental viscosity.

The second problem lies in the difficulty of evaluating the integral (2.22) for a general collision kernel $B(|v|,\eta)$. Even under the assumption of (2.29), the collision term remains a two dimensional integral. For numerical solutions of the system, this entails a significant additional computational cost. For higher moments closure systems, the situation is even more intractable. In order to overcome these problems it was proposed in [12] that for all molecular interaction models one should replace the Boltzmann collision operator (2.19) with the BGK approximation

$$\mathcal{C}_{\text{BGK}}(F) = \frac{1}{\tau(\rho,\theta)}\big(\mathcal{E}(\rho,u,\theta) - F\big)\,, \tag{2.39}$$

with the relaxation time $\tau(\rho,\theta)$ given by

$$\tau(\rho,\theta) = \frac{\mu(\theta)}{\rho\theta}\,, \tag{2.40}$$

where $\mu(\theta)$ is the true physical viscosity, and again $\mathcal{E}(\rho,u,\theta)$ is the Maxwellian density defined in (2.6). From the direct evaluation of (2.14), the resulting collision term for the Gaussian closure will then be

$$\Xi(\rho,\Theta) = \frac{\rho}{\tau(\rho,\theta)}\big(\theta I - \Theta\big) = \frac{\rho^2\theta}{\mu(\theta)}\big(\theta I - \Theta\big)\,. \tag{2.41}$$

A comparison with (2.34) and (2.37) shows that the BGK approximation recovers the leading order behavior of the Gaussian closure system near equilibrium, with the exception that the true viscosity now appears instead of the Gaussian viscosity $\mu_G$. Thus the BGK approximation automatically resolves the viscosity modification question discussed above by hardwiring the true physical viscosity in to the equation for $\Xi(\rho,\Theta)$. The form (2.39) was proposed for its simplicity. Based on the discussion following (2.28), one could more generally consider letting $\tau$ in (2.39) depend symmetrically on the eigenvalues of $\Theta$ so as to recover (2.40) when $\Theta = \theta I$. We will not consider such generalizations here.

### 2.4. Gaussian Closure for Maxwell Molecules

We now consider the special case of Maxwell molecules, for which the integral of (2.22) may be evaluated explicitly. A Maxwell molecule is generally a particle for which the collision kernel $B(|v|,\eta)$ is independent of $|v|$. This corresponds to the exponent $\gamma = 0$ in (2.29). This type of molecular interaction was first proposed by Maxwell [14] because of the great simplification it afforded in the analysis of the Boltzmann equation. This model appears frequently in the literature for this reason, e.g. [3]. For the Gaussian closure there is a

particular advantage to considering Maxwell molecules; namely, the difficulties discussed in the last section disappear. In particular, as was mentioned in the last section, the Gaussian viscosity and the true viscosity match exactly. Therefore, when the molecular interaction is chosen to be that of Maxwell molecules, a comparison of the Gaussian closure, the Navier-Stokes equations and the Boltzmann equation can be made without uncertainty regarding modifying the collisional parameters to obtain the true physical viscosity.

For Maxwell molecules, (2.22) simplifies to

$$\Xi(\rho,\Theta) = \frac{\kappa\,\rho^2}{m\sqrt{\det(4\pi\Theta)}} \int_{\mathbb{R}^3} \big(|v|^2 I - 3v\vee v\big)\, \exp\Big(-\tfrac{1}{4} v^T \Theta^{-1} v\Big)\, d^3\!v\,, \tag{2.42}$$

where $\kappa$ was defined by (2.32). The integral in (2.42) is just a Gaussian integral of the type we evaluated to obtain (2.13). Direct evaluation of the collision term $\Xi$ then yields

$$\Xi(\rho,\Theta) = \lambda\rho^2\big(\theta I - \Theta\big)\,, \tag{2.43}$$

where the constant $\lambda$ (independent of $\rho$ and $\Theta$) is given by

$$\lambda = \frac{6\kappa}{m}\,, \tag{2.44}$$

which is consistent with (2.36) for $\gamma = 0$. The Gaussian closure system (2.13) for Maxwell molecules then becomes

$$\partial_t\rho + \nabla_x\cdot\big(\rho u\big) = 0\,, \tag{2.45a}$$

$$\partial_t(\rho u) + \nabla_x\cdot\big(\rho u\vee u + \rho\Theta\big) = 0\,, \tag{2.45b}$$

$$\partial_t\big(\rho u\vee u + \rho\Theta\big) + \nabla_x\cdot\big(\rho u\vee u\vee u + 3\rho\Theta\vee u\big) = \lambda\rho^2\big(\theta I - \Theta\big)\,. \tag{2.45c}$$

It is the validity of this system that will be explored in the next section.

Because $\mu = \mu_{_G}$ for Maxwell molecules, by (2.37) one has

$$\mu(\theta) = \frac{\theta}{\lambda}\,. \tag{2.46}$$

We thereby observe that (2.43) is exactly the same expression as (2.41), which was obtained from the BGK approximation. This fact is particularly significant for the following reason. In general, the BGK form of the collision term is valid only for flows very close to thermal equilibrium. The above derivation shows that for the Gaussian closure with Maxwell molecules, the BGK form is correct even if the Gaussian distribution function is far from equilibrium. This suggests that the BGK operator, generalized in [12] to include thermal as well as viscous relaxation time scales, may be a legitimate approximation to the collision term for use in higher moment closure systems. This would allow an otherwise intractable collision term to be easily evaluated and tuned to give the correct fluid dynamic limit behavior.

## 3. APPLICATION TO PLANAR SHOCKS

Even under the assumption of Maxwell molecules or the BGK approximation, the Gaussian closure forms a rather complicated system of ten equations (2.45). As a first step in analyzing this system, we present now a study of the one-dimensional, rotationally symmetric reduction of these equations. This is the appropriate reduction for computing the canonical example of the planar shock profile. The one-dimensional nature and lack of boundary conditions make the shock profile an ideal test case for comparing the Gaussian closure with other approximating systems (Euler and Navier-Stokes) as well as with the full Boltzmann equation.

In the one-dimensional, rotationally symmetric geometry, all variables are functions of time and a single spatial coordinate $x$. The flow velocity in the $x$ direction $u(x,t)$ may vary; the velocities $v, w$ in the orthogonal directions are set to zero. For the Gaussian closure there are two relevant temperatures: the temperature in the direction of flow $\theta_{11}$, and the temperature in the orthogonal directions $\theta_{22}$. Because the flow remains one-dimensional, there are no off diagonal temperature components of the temperature matrix $\Theta$, i.e. $\theta_{12} = 0$. In this case (2.45) reduces to a system of four equations for $(\rho, u, \theta_{11}, \theta_{22})$

$$\begin{aligned}
\partial_t \rho + \partial_x(\rho u) &= 0\,, \\
\partial_t(\rho u) + \partial_x(\rho u^2 + \rho\theta_{11}) &= 0\,, \\
\partial_t(\rho u^2 + \rho\theta_{11}) + \partial_x(\rho u^3 + 3\rho u\theta_{11}) &= -\tfrac{2}{3}\lambda\rho^2(\theta_{11} - \theta_{22})\,, \\
\partial_t(\rho\theta_{22}) + \partial_x(\rho u\theta_{22}) &= \tfrac{1}{3}\lambda\rho^2(\theta_{11} - \theta_{22})\,.
\end{aligned} \tag{3.1}$$

Much of the analysis of the one-dimensional Gaussian closure using the BGK approximation has been presented in [5]. There the eigenstructure of the system (3.1) is investigated and a dispersion analysis is conducted. As shown in [5] there exist two genuinely nonlinear acoustic waves with wave speeds $u \pm \sqrt{3}c$, where $c = \sqrt{\theta_{11}}$. This indicates that when the flow satisfies $|u|/c > \sqrt{3}$, shocks will form.

We present here a complimentary analysis of the one-dimensional Gaussian closure system by deriving an exact analytic solution for the steady planar shock profile problem. As we shall see, for weak shocks for which at the upstream boundary we have $|u|/c < \sqrt{3}$, the two end states are connected by a smooth profile. For stronger shocks, the end states are connected by a jump discontinuity (shock) and a smooth profile. This corresponds to the results obtained in [5]. For our purposes, it is more convenient to introduce the change of variables

$$\theta = \tfrac{1}{3}(\theta_{11} + 2\theta_{22})\,, \qquad \sigma = \tfrac{1}{3}(\theta_{11} - \theta_{22})\,. \tag{3.2}$$

The new variables are the scalar temperature $\theta$ and a skew temperature $\sigma$ which measures the deviation of the system from thermodynamic equilibrium. At equilibrium, the skew

temperature vanishes and $\theta = \theta_{11} = \theta_{22}$. In these variables, the Gaussian closure becomes

$$\begin{aligned} \partial_t \rho + \partial_x(\rho u) &= 0\,, \\ \partial_t(\rho u) + \partial_x(\rho u^2 + \rho\theta + 2\rho\sigma) &= 0\,, \\ \partial_t(\tfrac{1}{2}\rho u^2 + \tfrac{3}{2}\rho\theta) + \partial_x(\tfrac{1}{2}\rho u^3 + \tfrac{5}{2}\rho u\theta + 2\rho u\sigma) &= 0\,, \\ \partial_t(\rho(\theta - \sigma)) + \partial_x(\rho u(\theta - \sigma)) &= \lambda\rho^2\sigma\,. \end{aligned} \tag{3.3}$$

Note that the first three equations, representing conservation of mass, momentum and energy, reduce to the Euler equations upon setting $\sigma = 0$, its equilibrium value.

This section is organized as follows. First we present a brief description of the shock structure problem, defining the Mach number and mean free path. Then the exact analytic solution for the steady planar shock profile is derived from the system (3.3). Next a short discussion of the Navier-Stokes and Boltzmann solutions for the shock problem is provided. The zero heat flux Navier-Stokes system (obtained from setting the thermal conductivity to zero) is also considered here. Finally, a comparison of the Gaussian, Navier-Stokes (with and without heat flux) and Boltzmann solutions is presented for weak and strong shocks.

### 3.1. The Shock Structure Problem

The planar shock is characterized by upstream (subscript $U$) and downstream (subscript $D$) equilibria $\mathcal{E}$ which are connected by a profile along which the fluid densities vary. In the stationary coordinate frame of the shock, the conservation laws dictate that the mass, momentum and energy fluxes must be constant along the profile. In particular, this means that the upstream and the downstream equilibria may be connected through the Rankine-Hugoniot relations

$$\begin{aligned} \rho_U u_U &= \rho_D u_D\,, \\ \rho_U u_U^2 + \rho_U \theta_U &= \rho_D u_D^2 + \rho_D \theta_D\,, \\ \tfrac{1}{2}u_U^2 + \tfrac{5}{2}\theta_U &= \tfrac{1}{2}u_D^2 + \tfrac{5}{2}\theta_D\,. \end{aligned} \tag{3.4}$$

A stationary planar shock may be described by two parameters, the Mach number Ma, which scales the dependent variables, and the mean free path $\ell$, which scales the independent position variable.

The local Mach number is defined at each point in the shock profile by

$$\mathrm{Ma} = \frac{|u|}{\sqrt{\frac{5}{3}\theta}}\,. \tag{3.5}$$

This is bounded above by $\mathrm{Ma}_U$, its value at the upstream equilibrium. The local Mach number decreases through the shock and achieves its smallest value at the downstream equilibrium, where it lies between 1 and $1/\sqrt{5}$ (these are the limiting values for an infinitely

weak and an infinitely strong shock). With the help of (3.4), the ratios of the downstream to upstream density, velocity, and temperature may be expressed solely as functions of $\mathrm{Ma}_U$ by

$$\begin{aligned}
\frac{\rho_D}{\rho_U} &= \frac{4\mathrm{Ma}_U^2}{\mathrm{Ma}_U^2+3}, \\
\frac{u_D}{u_U} &= \frac{\mathrm{Ma}_U^2+3}{4\mathrm{Ma}_U^2}, \\
\frac{\theta_D}{\theta_U} &= \frac{\left(\mathrm{Ma}_U^2+3\right)\left(5\mathrm{Ma}_U^2-1\right)}{16\mathrm{Ma}_U^2}.
\end{aligned} \tag{3.6}$$

Thus the shock strength is specified by the upstream Mach number, which is typically referred to simply as the Mach number of the shock. For an infinitely weak shock $\mathrm{Ma}_U = 1$; it increases without bound as the shock strength increases.

The mean free path $\ell$ is defined as the average distance a gas molecule travels between collisions. Because the changes through the shock profile occur due to collisions, this is a natural choice for the length scale. For a gas at equilibrium, the microscopic mean free path may be defined in terms of macroscopic parameters. The exact nature of the relationship depends on the collision kernel $B$ in (2.19). In the following we will use Bird's Variable Hard Sphere model [1] which assumes $B$ to be of the form (2.29) with $\beta(\eta)$ given by

$$\beta(\eta) = \frac{2\,m\,\theta_{\mathrm{ref}}}{\pi\,\mu_{\mathrm{ref}}}\,\eta\,. \tag{3.7}$$

Here $\mu_{\mathrm{ref}}$ is the viscosity at temperature $\theta_{\mathrm{ref}}$. For Maxwell molecules it follows that the viscosity coefficient $\mu$ has the form

$$\mu = \mu_{\mathrm{ref}}\,\frac{\theta}{\theta_{\mathrm{ref}}}, \tag{3.8}$$

so that by (2.46), the parameter $\lambda$ in the Gaussian closure is given by

$$\lambda = \frac{\theta_{\mathrm{ref}}}{\mu_{\mathrm{ref}}}. \tag{3.9}$$

We set the mean free path $\ell$ to be

$$\ell = \frac{\mu}{\rho\sqrt{\theta}}. \tag{3.10}$$

Here we have left off the factor of $\sqrt{2/\pi}$ which usually appears in the definition of mean free path for this model [2] in the interest of simplifying the equations. As we only use the mean free path to scale the position variable $x$, this factor is not important.

### 3.2. The Gaussian Closure System Shock Profile

We now consider the Gaussian closure system for a planar shock moving at a constant speed. In a coordinate reference frame moving at the speed of the shock, the shock is stationery, and the time derivatives of (3.3) vanish. It is convenient to choose as the reference state for the temperature, viscosity and mean free path the upstream equilibrium state. We then scale the position variable $x$ equations (3.3) by the upstream mean free path $\ell_U$ to obtain the dimensionless independent variable $X = x/\ell_U$. With the help of (3.9) the system (3.3) then becomes

$$\begin{aligned} \frac{d}{dX}(\rho u) &= 0\,, \\ \frac{d}{dX}(\rho u^2 + \rho\theta + 2\rho\sigma) &= 0\,, \\ \frac{d}{dX}(\tfrac{1}{2}\rho u^3 + \tfrac{5}{2}\rho u\theta + 2\rho u\sigma) &= 0\,, \\ \frac{d}{dX}(\rho u(\theta - \sigma)) &= \frac{\sqrt{\theta_U}}{\rho_U}\,\rho^2\sigma\,. \end{aligned} \tag{3.11}$$

The boundary conditions for this system of ODEs are given at $X = -\infty$ (upstream) and $X = \infty$ (downstream). These conditions are given in terms of $\rho_U$, $\theta_U$ and $\mathrm{Ma}_U$ by (3.5), (3.6) and

$$\sigma_U = 0\,, \qquad \sigma_D = 0\,. \tag{3.12}$$

The first three equations of (3.11) are easily solved using (3.5), (3.6) and (3.12) to give

$$\begin{aligned} C_1 &= \rho u = \rho_U u_U\,, \\ C_2 &= \rho u^2 + \rho\theta + 2\rho\sigma = \tfrac{1}{3}\rho_U\theta_U\left(5\mathrm{Ma}_U^2 + 3\right), \\ C_3 &= \tfrac{1}{2}\rho u^3 + \tfrac{5}{2}\rho u\theta + 2\rho u\sigma = \tfrac{5}{6}\rho_U u_U\theta_U\left(\mathrm{Ma}_U^2 + 3\right). \end{aligned} \tag{3.13}$$

These algebraic equations may be solved to give $u, \theta$ and $\sigma$ as functions of $\rho$ and the parameters $\rho_U$, $\theta_U$ and $\mathrm{Ma}_U$. These may then be substituted in to the last equation of (3.11) to give a single scalar ODE for $\rho(X)$. After some simplification, this ODE may be written

$$\frac{d\rho}{dX} = C\,\frac{\rho^3(\rho - \rho_U)(\rho_D - \rho)}{\rho - \rho_c}\,. \tag{3.14}$$

Here $\rho_c$ is a critical value for the density given by the formula

$$\rho_c = \frac{5}{3}\,\frac{4\mathrm{Ma}_U^2}{5\mathrm{Ma}_U^2 + 3}\,\rho_U\,. \tag{3.15}$$

For all shocks ($\mathrm{Ma}_U > 1$) we have that $\rho_c < \rho_D$. If it is also true that $\rho_c < \rho_U$, then (3.14) has a unique smooth solution connecting the end states $\rho_U$ and $\rho_D$. From (3.15)

this corresponds weak shocks with $\mathrm{Ma}_U < 3/\sqrt{5}$, which is equivalent to $|u_U|/\sqrt{\theta_U} < \sqrt{3}$. This was the criterion mentioned above for smooth solutions. It simply states that as long as the shock speed is smaller that the acoustic wave speed of the system, the solution will be smooth. For $\mathrm{Ma}_U > 3/\sqrt{5}$ it is necessary to look for a weak solution involving a smooth profile and a jump discontinuity such that the system (3.11) is weakly satisfied. The constant $C$ in (3.14) is expressed in terms of the boundary condition constants of (3.13) and the constant factor from (3.11) as

$$C = \frac{\sqrt{\theta_U}}{\rho_U}\,\frac{2C_3}{9C_1^2C_2} = \sqrt{\frac{5}{27}}\,\frac{1}{\rho_U^3}\,\frac{\mathrm{Ma}_U^2+3}{\mathrm{Ma}_U\left(5\mathrm{Ma}_U^2+3\right)}\,. \tag{3.16}$$

Here the shock has been chosen so that $u > 0$, and thus $C > 0$. From (3.14) we see that for $\rho_D > \rho > \max(\rho_c, \rho_U)$, $\rho(X)$ is an increasing function, as expected. Moreover, we can in fact integrate (3.14) exactly to give the position coordinate $X$ as a function of $\rho$

$$\begin{aligned} X(\rho) &= \frac{1}{C}\int \frac{\rho-\rho_c}{\rho^3(\rho-\rho_U)(\rho_D-\rho)}\,d\rho \\ &= A_1\log(\rho) + A_2\frac{1}{\rho} + A_3\frac{1}{\rho^2} + A_4\log(\rho-\rho_U) + A_5\log(\rho_D-\rho)\,, \end{aligned} \tag{3.17}$$

where the constants are

$$\begin{aligned} A_1 &= \frac{1}{C}\left(-\frac{\rho_U+\rho_D+\rho_c}{(\rho_U\rho_D)^2} + \frac{\rho_c(\rho_U+\rho_D)^2}{(\rho_U\rho_D)^3}\right), \\ A_2 &= \frac{1}{C}\left(\frac{1}{\rho_U\rho_D} - \frac{\rho_c(\rho_U+\rho_D)}{(\rho_U\rho_D)^2}\right), \\ A_3 &= -\frac{1}{C}\left(\frac{\rho_c}{2\rho_U\rho_D}\right), \\ A_4 &= -\frac{1}{C}\left(\frac{\rho_c-\rho_U}{\rho_U^3(\rho_D-\rho_U)}\right), \\ A_5 &= -\frac{1}{C}\left(\frac{\rho_D-\rho_c}{\rho_D^3(\rho_D-\rho_U)}\right). \end{aligned} \tag{3.18}$$

Note that an arbitrary constant may be added to $X(\rho)$. This corresponds to the fact that there is no fixed coordinate label for the shock profile inherent in the problem. We shall find it convenient to choose this constant such that $X = 0$ corresponds to the "equal area point" for density. This is the point $X^*$ such that

$$\int_{-\infty}^{X^*} (\rho(X)-\rho_U)\,dX = \int_{X^*}^{\infty} (\rho_D-\rho(X))\,dX\,. \tag{3.19}$$

The validity of (3.17) as a solution to (3.11) depends on the Mach number. For weak shocks with $\mathrm{Ma}_U < 3/\sqrt{5}$, (3.17) is valid for all $\rho_U < \rho < \rho_D$. This gives a smooth profile

which connects the upstream and downstream equilibrium states. For stronger shocks with $\mathrm{Ma}_U > 3/\sqrt{5}$, $\rho_c > \rho_U$ and the solution (3.17) is only valid for $\rho_c < \rho < \rho_D$. To connect to the upstream equilibrium state requires the introduction of a jump. Such a solution may be described as follows. To the left of the jump (upstream) set the solution to be the constant upstream equilibrium state. The first three jump conditions associated with (3.11) are automatically satisfied by any solution of (3.14) simply by definition of $u, \theta$ and $\sigma$ as functions of $\rho$. There remains, however, an additional constraint corresponding to the fourth equation. In order for this equation to be weakly satisfied across a jump it is necessary that the condition

$$\left[\rho u(\theta - \sigma)\right]_{\text{Left}} = \left[\rho u(\theta - \sigma)\right]_{\text{Right}} \tag{3.20}$$

hold, where the subscripts Left and Right indicate evaluation of the expression on either side of the jump. The first equation of (3.11) shows that $\rho u$ is constant across the jump (conservation of mass); thus this factor may be canceled from (3.20), which then becomes

$$\left[\theta - \sigma\right]_{\text{Left}} = \left[\theta - \sigma\right]_{\text{Right}} . \tag{3.21}$$

The left state is the upstream equilibrium, for which $\sigma = 0$. Using the subscript $s$ (for shock) to denote the right state after the jump, (3.21) states that

$$\theta_U = \theta_s - \sigma_s . \tag{3.22}$$

With the help of (3.13), this relationship may be rewritten in terms of density as

$$\rho_s = \frac{10\mathrm{Ma}_U^2}{5\mathrm{Ma}_U^2 + 9}\,\rho_U . \tag{3.23}$$

We see from (3.15) that for $\mathrm{Ma}_U > 3/\sqrt{5}$ we have

$$\rho_U < \rho_c < \rho_s < \rho_D . \tag{3.24}$$

Thus the upstream equilibrium may be connected by a jump to the shock state $s$ given by (3.23), which then may be connected to the downstream equilibrium with the profile given by (3.17). For the weakest shock for which a jump is necessary, the ratio of the Gaussian jump $\rho_s$ to the Euler (downstream) jump $\rho_D$ is 2/3. This decreases as Mach number increases. In the limit of an infinite strength shock, $\rho_s/\rho_D = 1/2$. Thus, even when a weak solution jump is required, the Gaussian closure still gives a significant profile.

### 3.3. The Navier-Stokes and Boltzmann Profiles

The standard fluid dynamic system for compressible gas flows is the Navier-Stokes equations. Under the same scalings as above for the Gaussian closure, the Navier-Stokes system reduces to the coupled ODE system

$$\begin{aligned} \tfrac{4}{3}\theta \frac{du}{dX} &= C_1 \frac{1}{u}(u^2+\theta) - C_2 \,, \\ \tfrac{15}{4}\theta \frac{d\theta}{dX} &= C_1 \left( \tfrac{3}{2}\theta - \tfrac{1}{2}u^2 + \frac{C_2}{C_1} u \right) - C_3 \,. \end{aligned} \tag{3.25}$$

Here the constants are again given by (3.13). The temperature $\theta$ which appears before the derivatives plays the role of the viscosity and thermal conductivity. This follows from the fact that the molecular model satisfies (3.8) and has a constant Prandtl number of 2/3.

The system (3.25) does not have an exact solution in terms of elementary functions. However, following the classical procedure of Gilbarg and Paolucci [8], we may integrate the system numerically to obtain the smooth shock profile solution.

As described in Section 2, the Gaussian closure system shows viscous effects, but has no heat flux. This suggests that the Navier-Stokes equations with the thermal conductivity set identically equal to zero would be perhaps the most natural system with which to compare the Gaussian closure. In the fluid dynamic limit, one would expect the two systems, having equal transport coefficients (for the case of Maxwell molecules), to be very close. We therefore include the zero heat flux ($q = 0$) Navier-Stokes equation in our comparison of shock profiles.

As in the case of the Gaussian closure, we can derive an exact analytic profile for the $q = 0$ Navier-Stokes system. This is obtain by setting the second equation of the system (3.25) to zero. The first equation then becomes an ODE for velocity, which, by the conservation of mass, may be rewritten as an equation for density. The result, which may be compared to (3.14), is

$$\frac{d\rho}{dX} = C_{NS} \frac{\rho^3 (\rho - \rho_U)(\rho_D - \rho)}{(\rho - \rho_a)^2 + \rho_b^2} \,. \tag{3.26}$$

Here the constants $C_{NS}$, $\rho_a$ and $\rho_b$ are given by

$$\begin{aligned} C_{NS} &= \sqrt{\frac{27}{80}} \frac{1}{\rho_U^2} \mathrm{Ma}_U \,, \\ \rho_a &= \frac{\rho_U + \rho_D}{5} \,, \\ \rho_b &= \frac{3}{5} \frac{\sqrt{5\mathrm{Ma}_U^2 - 1}}{(\mathrm{Ma}^2 + 3)} \rho_U \,. \end{aligned} \tag{3.27}$$

It can be seen in (3.26) that, unlike (3.14), the denominator is never zero. Thus the solution of (3.26) will be a smooth profile for all Mach numbers. However, as the Mach

number increases, $\rho_b^2$ will approach zero while $\rho_a$ approaches $\rho_U$. This indicates that sharp gradients can be expected from densities near the upstream equilibrium at large Mach numbers.

As above, the equation (3.26) may be integrated exactly to give the position coordinate $X_{NS}^{q=0}$ as a function of $\rho$

$$\begin{aligned} X_{NS}^{q=0}(\rho) &= \frac{1}{C_{NS}} \int \frac{(\rho-\rho_a)^2+\rho_b^2}{\rho^3(\rho-\rho_U)(\rho_D-\rho)}\, d\rho \\ &= B_1 \log(\rho) + B_2 \frac{1}{\rho} + B_3 \frac{1}{\rho^2} + B_4 \log(\rho-\rho_U) + B_5 \log(\rho_D-\rho)\,, \end{aligned} \tag{3.27}$$

where the constants are

$$\begin{aligned} B_1 &= \frac{1}{C_{NS}} \left( -\frac{1}{\rho_U \rho_D} + \frac{\rho_a^2+\rho_b^2+2\rho_a(\rho_U+\rho_D)}{(\rho_U \rho_D)^2} - \frac{(\rho_a^2+\rho_b^2)(\rho_U+\rho_D)^2}{(\rho_U \rho_D)^3} \right), \\ B_2 &= \frac{1}{C_{NS}} \left( -\frac{2}{\rho_U \rho_D} + \frac{(\rho_a^2+\rho_b^2)(\rho_U+\rho_D)}{(\rho_U \rho_D)^2} \right), \\ B_3 &= \frac{1}{C_{NS}} \left( \frac{(\rho_a^2+\rho_b^2)}{2\rho_U \rho_D} \right), \\ B_4 &= \frac{1}{C_{NS}} \left( \frac{(\rho_U-\rho_a)^2+\rho_b^2}{\rho_U^3(\rho_D-\rho_U)} \right), \\ B_5 &= -\frac{1}{C_{NS}} \left( \frac{(\rho_D-\rho_a)^2+\rho_b^2}{\rho_D^3(\rho_D-\rho_U)} \right). \end{aligned} \tag{3.28}$$

As before, a constant is added to the position so that $X_{NS}^{q=0} = 0$ is the equal area point for the density profile.

The Boltzmann shock profile is computed using the Direct Simulation Monte Carlo method developed by Bird [1]. The DSMC method is a particle simulation in which particles convect independently over a time step $\Delta t$. They are then grouped into cells of size $\Delta x$. Pairs of particles within each cell undergo collisions with a probability proportional to their relative velocities (or a power thereof) and $\Delta t$. For Maxwell molecules, the simulation becomes particularly simple because the probability of a pair colliding is independent of relative velocity. The convection and collision steps are alternated until a steady state is achieved and an adequate sample size is collected. Macroscopic quantities such as density and stream velocity are computed as cell averages.

For the current simulation of the steady planar shock wave, the spatial domain was taken to be one dimension, while the fully three dimensional velocity space was retained. The cell size, which was constant through the domain, was chosen to be

$$\Delta x = \frac{1}{20}\, \ell_U\,, \tag{3.29}$$

where $\ell_u$ is the upstream mean free path. The time step was taken to be

$$\Delta t = \frac{1}{10} \frac{\Delta x}{\sqrt{2\theta_u}}. \tag{3.30}$$

For the Mach number considered, the fastest particles (those with velocities on the order of $|u_u| + 3\sqrt{3\theta_u}$, where $u_u$ is the upstream stream velocity) travel approximately one cell in one time step. This is within the DSMC guidelines.

The collision step was computed using Bird's NTC algorithm with the Variable Hard Sphere collision model. Because the Maxwell molecule model was used, there was no need to apply the usual rejection technique for this simulation (i.e., all collision pairs are accepted).

The stationary shock profile was computed with a time dependent simulation starting from initial data consisting of the domain divided equally into the two constant states. Initially, the upstream cells contained 200 simulation particles. The initial particle velocities were sampled from a Maxwellian distribution with the density, stream velocity and temperature of the associated constant state. Incoming particles at both ends were sampled from the corresponding flux weighted Maxwellian distributions. Additionally, a "shock stabilizing" scheme was used at the boundary to ensure that neither to few or too many particles left the domain in a given time step. This essentially held the shock in a fixed position, minimizing the smearing out effect associated with a random drift of the shock position. The number of cells used varied with the Mach number. The simulation was run until a steady state was reached. The velocity averages were then collected by running the simulation another 30000 time steps and sampling the cell data every third time step.

### 3.4. Comparison of Shock Profiles

We now compare the solution of the Gaussian closure system described in Section 3.2 with the computed Navier-Stokes and Boltzmann shock profiles as well as with the zero heat flux Navier-Stokes profile. Several flow regimes, determined by the Mach number, are considered. First, a Mach 1.2 shock is presented as a typical weak shock which is frequently studied in the literature [1], [4]. This represents a near equilibrium flow for which fluid dynamic descriptions should be valid. Next Mach $1.34 \approx 3/\sqrt{5}$ is presented as the flow for which the singularity for the Gaussian closure first develops. Mach 3 is chosen as a flow for which there is significant breakdown of the fluid dynamic description. An investigation of the breakdown of the Navier-Stokes system as Mach number increases can be found in [13]. Finally results for Mach 9 are given. This corresponds to a strong shock in the middle of which the gas is quite far from thermodynamic equilibrium so that the assumptions underlying the derivation of the Navier-Stokes system from the Boltzmann equation are no longer valid.

In Figure 1 the density profiles for the four Mach numbers are shown. In order to facilitate a comparison across Mach numbers, we plot the relative density defined by

$$\widehat{\rho} = \frac{\rho - \rho_U}{\rho_D - \rho_U} . \tag{3.31}$$

The coordinate $x = 0$ is chosen as the equal area point defined by (3.19) for all the graphs. The Gaussian closure and $q = 0$ Navier-Stokes density profiles are seen to be quite close for low Mach numbers, as expected. However, even at the low Mach numbers, the Gaussian closure is seen to be slightly better at capturing the true fluid behavior. This indicates that treating temperature as a symmetric, positive definite variance matrix, as opposed to a scalar quantity, leads to a more accurate description of the near equilibrium flow, given the restriction of zero heat flux. We therefore expect that higher moment systems, which include heat flux effects, to yield better results in this regime than the standard fluid approximation. The improvement, will only be slight at low Mach numbers, however, because as can be seen from the graphs, the full Navier-Stokes and Boltzmann profiles are also nearly identical for low $\mathrm{Ma}_U$. The discrepancy between the two sets can be viewed as a measure of the influence of heat flux on near equilibrium flows.

At higher Mach numbers, the situation changes. As is well known, the full Navier-Stokes profile no longer accurately models the Boltzmann profile. The zero heat flux Navier-Stokes develops large gradients near the upstream equilibrium, as expected, but shows significant deviations from the Gaussian closure profile. Surprisingly, the Gaussian closure profile shows quite accurate agreement with the full Navier-Stokes profile downstream of the equal area point. This again indicates that the multiple temperature Gaussian closure captures more of the physics than its missing heat flux component might suggest, and that higher moment closure systems will describe more closely the true non-equilibrium nature of the flow.

The temperature profiles are given in Figure 2. Again we plot a scaled temperature defined by

$$\widehat{\theta} = \frac{\theta - \theta_U}{\theta_D - \theta_U} , \tag{3.32}$$

The effects of heat flux in the Boltzmann and Navier-Stokes equations can clearly be seen as the temperature profiles considerably lead the density profiles. This effect does not appear for the Gaussian profile or $q = 0$ Navier-Stokes profile.

As a last comparison, we consider the skew temperature $\sigma$. This may be defined in terms of the underlying kinetic velocity distribution function as

$$\rho\sigma = \tfrac{1}{3} \int_{\mathbb{R}^3} \left[ (v_x - u_x)^2 - \tfrac{1}{2}\left( (v_y - u_y)^2 + (v_z - u_z)^2 \right) \right] F(v)\, d^3v . \tag{3.33}$$

Here $u = (u_x, u_y, u_z)$ is the stream velocity, which is the average with respect to $F$ of the particle velocity $v = (v_x, v_y, v_z)$. When the Gaussian distribution function (2.11) is

used to evaluate (3.33) with the $\Theta$ described by (3.2), (3.33) becomes an identity for $\sigma$. If the Chapman-Enskog distribution function [6], from which the Navier-Stokes equations are obtained, is inserted in (3.33), the result is

$$\rho\sigma_{NS} = -\tfrac{2}{3}\mu\frac{du}{dx} = -\tfrac{1}{2}\left(C_1\frac{1}{u}(u^2+\theta) - C_2\right). \tag{3.34}$$

The definition (3.33) can also be used in the Monte Carlo simulation of the Boltzmann equation to compute $\sigma$. For the $q = 0$ Navier-Stokes profile, (3.34) is taken as the definition of $\sigma_{NS}^{q=0}$. A comparison of the values of $\sigma$ for the various profiles is given in Figure 3. From these graphs we see that the correct physical value for $\sigma$, given by the Boltzmann equation solution, is smaller than the values obtained from the other models. It can be seen that the inclusion of heat flux effects lowers $\sigma$. Between the Gaussian closure and the $q = 0$ Navier-Stokes profiles, the Gaussian closure $\sigma$ tends to be smaller, suggesting again that it is the more physial of the two, and that once heat flux is introduced into a moment closure system, a more accurate description of the flow will be obtained.

## 4. CONCLUSIONS

The Euler equations, related to the Maxwellian closure for the Boltzmann moment equations, are the first member of a hierarchy of moment closure systems which may be derived systematically from the Boltzmann equation [12]. This paper has investigated the next member of this family, the Gaussian closure. Here we reduce the 8 dimensional collision integral to an integral over $\mathbb{R}^3$, which, under a common assumption on the collision kernal, further reduces to an integral over the unit sphere. For the special case of Maxwell molecules, this integral may be evaluated exactly to give a simple expression for the collision term. This term is seen to be identical to the term obtained for the Gaussian closure using the BGK approximation to the collision operator, independent of how far the system is from thermal equilibrium. This suggests that the BGK approximation may be a reasonable means of simplifying the collision term for subsequent members of the moment closure systems hierarchy. Other results concerning the Gaussian closure appear in [12], [5].

The Gaussian closure for Maxwell molecules is studied for the special case of a steady planar shock profile. The system is reduced to an autonomous ODE for the density $\rho(X)$, which may then be solved explicitly to express the inverse function $X(\rho)$ in terms of elementary functions of $\rho$. The key parameter in the equation is the Mach number $\mathrm{Ma}_U$, which describes the shock strength. It is seen that for weak shocks with $\mathrm{Ma}_U < 3/\sqrt{5}$, the Gaussian solution is a smooth profile which connects the equilibrium end states. For shocks with $\mathrm{Ma}_U > 3/\sqrt{5}$, the Gaussian closure requires a weak solution connecting the end states with a smooth profile linked to a jump. The necessity of weak solutions is a feature of all the systems of the hierarchy. The results here show that even for large Mach numbers, these systems still lead to a significant shock profile.

A comparison with the Navier-Stokes profile and the Boltzmann equation solution shows that the Gaussian closure provides a reasonably accurate description for weak shocks. The key component missing from the Gaussian closure is heat flux. A comparison of the Gaussian closure with the zero heat flux Navier-Stokes equation, obtained by setting the thermal conductivity to zero, shows that the Gaussian closure is in general superior, with the degree of improvement increasing with Mach number. We anticipate that for higher moment closure systems, which include heat flux, a similar improvement over the full Navier-Stokes system will be obtained where the moment closure solution is smooth. For stronger shocks, the Gaussian closure density profile downstream of the equal area point accurately matches the Navier-Stokes profile, whereas the zero heat flux Navier-Stokes profile is significantly different. We observe by monitoring the skew temperature $\sigma$ through the shock profile that the $q = 0$ Navier-Stokes equation gives a larger $\sigma$ than the Gaussian closure. The full Navier-Stokes system also leads to a $\sigma$ which is too large compared with the Boltzmann profile. This supports the assertion that higher moment closure systems will provide a better physical description of the flow.

The Gaussian closure investigated here is not intended to compete with the fluid dynamic equations. It is presented as a prototype of a system obtained from a nonperturbative closure for the Boltzmann equation which leads to a symmetric hyperbolic system of PDEs which possesses an entropy. The study of the shock structure and collision term of the Gaussian closure system is intended to facilitate investigations both of extentions of the Gaussian system [11] and of the considerably more complicated higher moment closure schemes which allow for heat flux as well as viscous effects [12], [9].

## Appendix: EVALUATION OF THE COLLISION TERM

The eight-fold integral of (2.21) has standard symmetries [6] under the exchange of the $v$ and $w$ variables and the exchange of the primed and unprimed variables, by which (2.21) can be brought into the form

$$\Xi(\rho,\Theta) = \frac{1}{m}\int_{\mathbb{R}^3}\int_{\mathbb{R}^3}\int_{\mathbb{S}^2_+} \tfrac{1}{2}\big(w'\vee w' + v'\vee v' - w\vee w - v\vee v\big)\,\mathcal{G}(v)\mathcal{G}(w)\,B\,d^2\hat{n}\,d^3\hat{w}\,d^3\hat{v}\,, \quad \text{(A.1)}$$

Below we will reduce the eight-fold integral above to the integral given in (2.22).

The first reduction of the integral in (A.1) is achieved after changing variables to the center of mass velocity coordinates. The pre-collision center of mass velocity $v_m$ and the relative velocity $v_r$ are defined as

$$v_m = \tfrac{1}{2}(v+w)\,, \qquad v_r = v - w\,. \quad \text{(A.2)}$$

The differential volume element for this change of variables satisfies $d^3\hat{v}_m\,d^3\hat{v}_r = d^3\hat{v}\,d^3\hat{w}$. It follows from (2.20) that the post-collision values of the center of mass and relative velocities are given by

$$v'_m = v_m\,, \qquad v'_r = v_r - 2n(n\cdot v_r)\,. \quad \text{(A.3)}$$

The velocities $v$, $w$, $v'$ and $w'$ maybe then be expressed as

$$\begin{aligned} v &= v_m + \tfrac{1}{2} v_r\,, \qquad & w &= v_m - \tfrac{1}{2} v_r\,, \\ v' &= v_m + \tfrac{1}{2} v_r'\,, \qquad & w' &= v_m - \tfrac{1}{2} v_r'\,. \end{aligned} \tag{A.4}$$

Upon using these relations, the first factor in the integrand of (A.1) then transforms to

$$\tfrac{1}{2}\big(w'\vee w' + v'\vee v' - w\vee w - v\vee v\big) = \tfrac{1}{4}\big(v_r'\vee v_r' - v_r\vee v_r\big)\,, \tag{A.5}$$

while, by (2.11), the second factor becomes

$$\begin{aligned} \mathcal{G}(v)\mathcal{G}(w) &\equiv \frac{\rho^2}{\det(2\pi\Theta)} \exp\Big( - \tfrac{1}{2} v^T \Theta^{-1} v - \tfrac{1}{2} w^T \Theta^{-1} w\Big) \\ &= \frac{\rho^2}{\det(2\pi\Theta)} \exp\Big( - v_m^T \Theta^{-1} v_m - \tfrac{1}{4} v_r^T \Theta^{-1} v_r\Big)\,. \end{aligned} \tag{A.6}$$

The integration over $v_m$ can then be carried out explicitly and (A.1) reduces to

$$\Xi(\rho,\Theta) = \frac{\rho^2}{m\,\sqrt{\det(4\pi\Theta)}} \int_{\mathbb{R}^3}\int_{\mathbb{S}^2_+} \tfrac{1}{4}\big(v_r'\vee v_r' - v_r\vee v_r\big)\, \exp\Big( - \tfrac{1}{4} v_r^T \Theta^{-1} v_r\Big)\, B\, d^2\hat{n}\, d^3 v_r\,. \tag{A.7}$$

which leaves a five-fold integral.

The next reduction is achieved by isolating the contribution to the $n$ integration in (A.7). Namely, (A.7) can be recast as

$$\Xi(\rho,\Theta) = \frac{\rho^2}{m\,\sqrt{\det(4\pi\Theta)}} \int_{\mathbb{R}^3} M(v_r)\,|v_r|^2\, \exp\Big( - \tfrac{1}{4} v_r^T \Theta^{-1} v_r\Big)\, d^3 v_r\,, \tag{A.8}$$

where $M(v_r)$ is the matrix-valued function defined by

$$M(v_r) \equiv \frac{1}{|v_r|^2} \int_{\mathbb{S}^2_+} \tfrac{1}{4}\big(v_r'\vee v_r' - v_r\vee v_r\big)\, B(|v_r|,\eta)\, d^2\hat{n}\,. \tag{A.9}$$

Note that $M(v_r)$ contains all the information about the collisional kernel $B$ and is independent of $\rho$ and $\Theta$. It is clear that $M(v_r)$ is a symmetric matrix. Because $|v_r'| = |v_r|$ by (A.3), it is traceless too. Moreover, also by (A.3), the matrix is invariant under conjugation by any rotation matrix that leaves the vector $v_r$ fixed. Hence, $M(v_r)$ must have the form

$$M(v_r) = \left( I - 3\frac{v_r\vee v_r}{|v_r|^2}\right)\, \xi(|v_r|)\,, \tag{A.10}$$

where the scalar-valued function $\xi(|v_r|)$ satisfies

$$\xi(|v_r|) = -\tfrac{1}{2}\frac{v_r^T M(v_r) v_r}{|v_r|^2} = \tfrac{1}{8}\int_{\mathbb{S}^2_+} \left(1 - \frac{(v_r\cdot v_r')^2}{|v_r|^4}\right) B(|v_r|,\eta)\, d^2\hat{n}\,. \tag{A.11}$$

Indeed, by (A.3) one has

$$\frac{(v_r \cdot v_r')}{|v_r|^2} = 1 - 2\frac{(n \cdot v_r)^2}{|v_r|^2} = 1 - 2\eta^2\,, \tag{A.12}$$

so that, recalling that $d^2\hat{n} = d\eta\, d\phi$, the integral in (A.11) becomes

$$\begin{aligned} \xi(|v_r|) &= \tfrac{1}{2}\int_0^{2\pi}\int_0^1 \left(\eta^2 - \eta^4\right) B(|v_r|,\eta)\, d\eta\, d\phi \\ &= \pi \int_0^1 \left(\eta^2 - \eta^4\right) B(|v_r|,\eta)\, d\eta\,. \end{aligned} \tag{A.13}$$

Hence, (A.8) can be expressed in terms of $\xi(|v_r|)$ through (A.10) as

$$\Xi(\rho,\Theta) = \frac{\rho^2}{m\sqrt{\det(4\pi\Theta)}} \int_{\mathbb{R}^3} \left(|v_r|^2 I - 3v_r \vee v_r\right) \xi(|v_r|)\, \exp\Big(-\tfrac{1}{4} v_r^T \Theta^{-1} v_r\Big)\, d^3\!v_r\,. \tag{A.14}$$

Formulas (2.22) and (2.23) then follow by simply replacing $v_r$ by $v$ in (A.14) and (A.13) respectively.

**Acknowledgments.**

C.D.L. was partially supported by the AFOSR under grant F49620-92-J-0054 at the University of Arizona. W.J.M was supported by the National Science Foundation through an NSF Postdoctoral Fellowship while at the University of Arizona and the University of California, Los Angeles.

## References

[1] G.A. Bird, *Molecular Gas Dynamics and the Direct Simulation of Gas Flows*, Oxford University Press, Oxford, 1994.

[2] G.A. Bird, *Definition of Mean Free Path for Real Gases*, Phys. Fluids., **26** (1983), pp. 3222.

[3] A.V. Bobylev, *Fourier Transform Method in the Theory of the Boltzmann Equation for Maxwell Molecules*, Soviet Physics Doklady, **20** (12) (1975), pp. 820-822.

[4] I. Boyd, G. Chen and G. Candler, *Predicting Failure of the Continuum Fluid Equations in Transitional Hypersonic Flows*, Phys. Fluids **7** (1) (1995), pp. 210-219.

[5] S.L. Brown, P.L. Roe, and C.P.T. Groth, *Numerical Solution of a 10-Moment Model for Nonequilibrium Gas Dynamics*, AIAA 12th Computational Fluid Dynamics Conference 1994.

[6] C. Cercignani, *The Boltzmann Equation and Its Applications*, Applied Mathematical Sciences **67**, Springer-Verlag, New York, 1988.

[7] S. Chapman and T.G. Cowling, *The Mathematical Theory of Non-Uniform Gases*, Third Edition, Cambrigde University Press, Cambrigde, 1970.

[8] D. Gilbarg and D. Paolucci, *The Structure of Shock Waves in the Continuum Theory of Fluids*, J. Rat. Mech. & Anal. **2** (1953), pp. 617-643.

[9] T.I. Gombosi, C.P.T. Groth, P.L. Roe, and S.L. Brown, *35-Moment Closure for Rarefied Gases: Derivation, Transport Equations, and Wave Structure*, Phys. Fluids (submitted 1994).

[10] H. Grad, *On the Kinetic Theory of Rarefied Gases*, Comm. Pure & Appl. Math. **2** (1949), pp. 331-407.

[11] C.P.T. Groth and C.D. Levermore, *Beyond the Navier-Stokes Approximation: Transport Corrections to the Gaussian Closure*, (in preparation 1996).

[12] C.D. Levermore, *Moment Closure Hierarchies for Kinetic Theories*, J. Stat. Phys. **83** (1996), pp. 1021-1065.

[13] C.D. Levermore, W.J. Morokoff and B.T. Nadiga, *Moment Realizability and the Validity of the Navier-Stokes Equations*, Physics of Fluids (submitted 1995).

[14] J.C. Maxwell, *On the Dynamical Theory of Gases*, Phil. Trans. Roy. Soc. London **157** (1866), 49–88; also in "The Scientific Papers of James Clerk Maxwell" **2**, Dover, New York, 1965, pp. 26–78.

[15] W.J. Morokoff and A. Kersch, *A Comparison of Scattering Angle Models*, Computers and Math. with Appl. (to appear 1996).

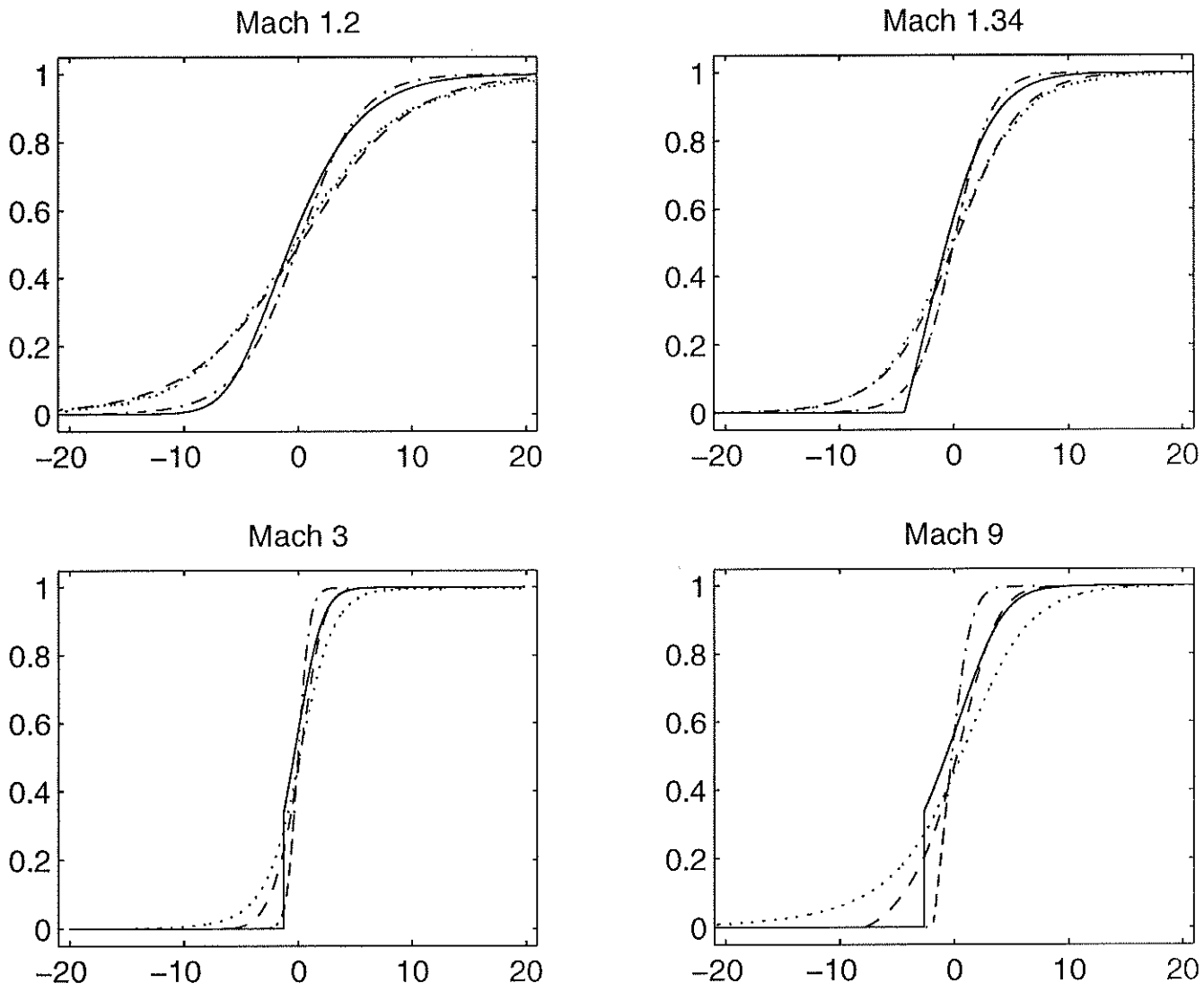


Figure 1: Scaled density profiles plotted as a function of the $X$ (distance scaled by the mean free path). The solid line is the Gaussian closure system solution. The dashed line is the Navier-Stokes solution. The dotted line is the Boltzmann solution. The dash-dot line is the Navier-Stokes solution with $q = 0$.

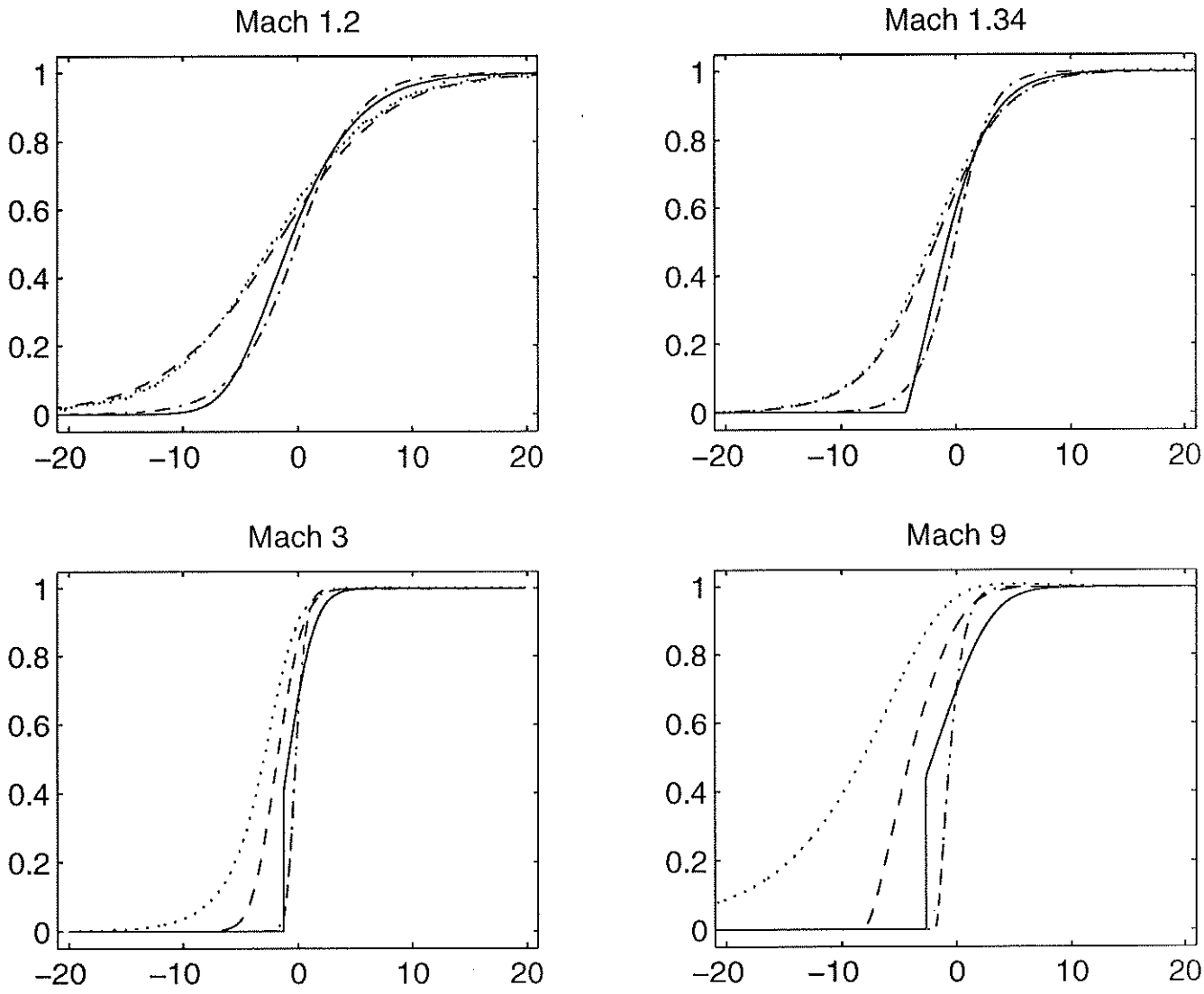


Figure 2: Scaled temperature profiles plotted as a function of the $X$ (distance scaled by the mean free path). The solid line is the Gaussian closure system solution. The dashed line is the Navier-Stokes solution. The dotted line is the Boltzmann solution. The dash-dot line is the Navier-Stokes solution with $q = 0$.

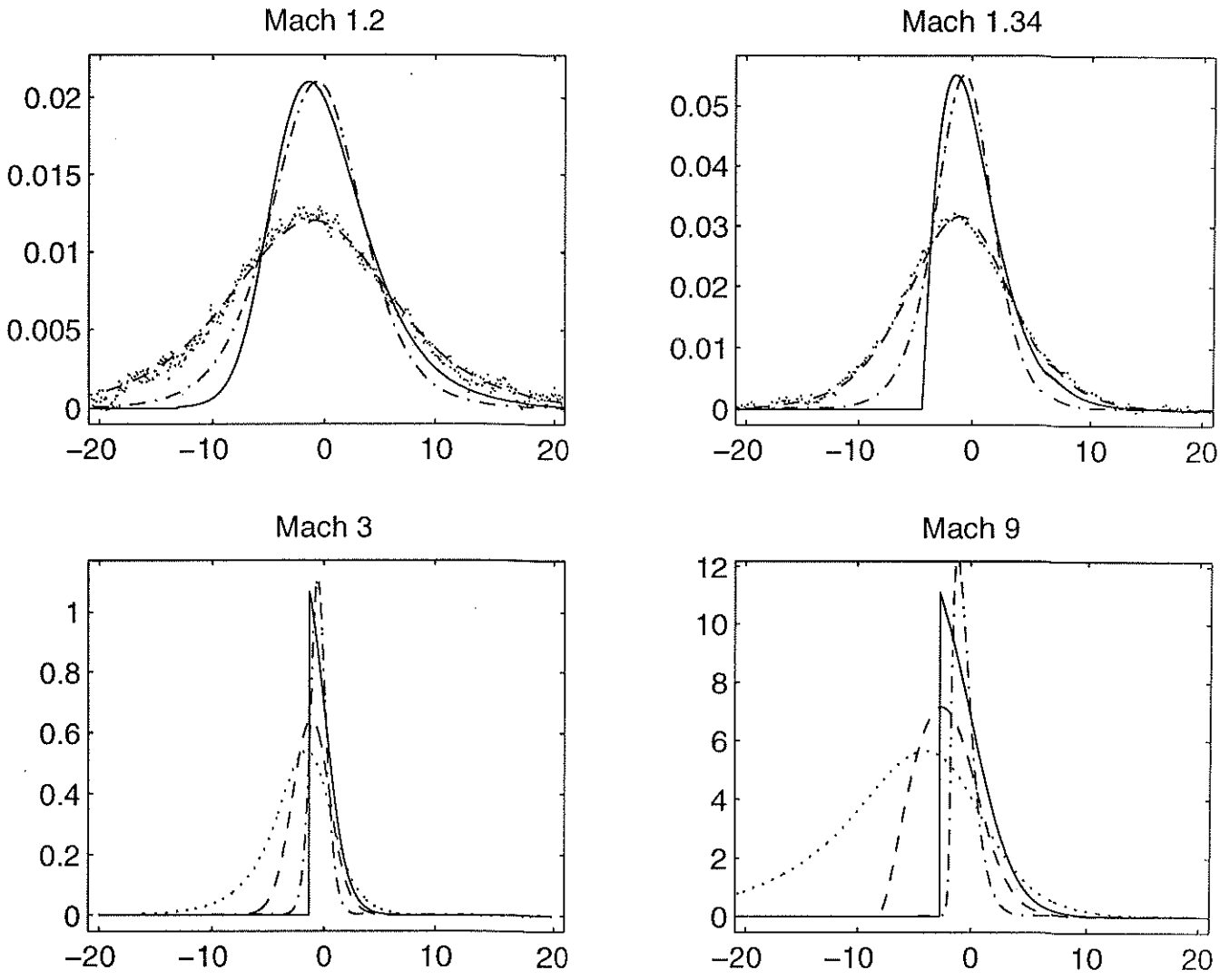


Figure 3: Skew temperature profiles plotted as a function of the $X$ (distance scaled by the mean free path). The solid line is the Gaussian closure system solution. The dashed line is the Navier-Stokes solution. The dotted line is the Boltzmann solution. The dash-dot line is the Navier-Stokes solution with $q = 0$.